

## **Seismic Rehabilitation of Substation Equipment by Friction Pendulum Systems**

\*Reza Karami Mohammadi<sup>1)</sup> and Erfan Mosaffa<sup>2)</sup>

<sup>1), 2)</sup> Department of Civil Engineering, K.N.Toosi University of Technology, Tehran, Iran  
1) rkarami@kntu.ac.ir

### **ABSTRACT**

Substation damage and consequently electricity cut off has been constantly one of the costly earthquake disastrous outcomes. In the present study, a 2-item set of equipment including capacitive voltage transformer (CVT) adjacent to a lightning arrester (LA), known as vulnerable instruments existing in substation, are aimed to seismically strengthen by isolation strategy. By taking advantage of incremental dynamic analysis (IDA) and then defining an appropriate damage state, equipment seismic response is measured. Subsequently, fragility functions are developed to evaluate the seismic performance of friction pendulum system (FPS). It revealed that the FPS isolator has the potential to decrease flexural stresses caused by intense ground motions which can be enhanced by widening the gap between stoppers of isolator. This approach results in postponing the porcelain breakage and makes electric power transmission more reliable in the event of a major earthquake.

**KEYWORDS:** friction pendulum system, lightning arrester, capacitor voltage transformer, porcelain breakage, incremental dynamic analysis, fragility curves.

### **I. INTRODUCTION**

Experience gained during recent earthquakes has demonstrated that an earthquake poses a major threat to substation equipment items [1]. Power outage can significantly impede the rescue operation in the crucial time following the disaster. Therefore, substations play an important role in electric power network [2]. For a reliable delivery of electricity immediately after an earthquake, these components must continue to function and any interruption or serious damage can lead to far-reaching consequences [3]. Loma Prieta (1989) and Northridge (1999) earthquakes caused over \$280 million damage to the USA power system facilities [4]. High voltage substations facilities received heavy damage induced by Kocaeli (1999) earthquake including 800 of MV/LV type transformers (7% of total inventory) in the affected urban areas [5]. Loshan

---

<sup>1)</sup> Professor

<sup>2)</sup> Graduate Student

substation (230 kV) had experienced failures of 23 disconnect switches, 11 circuit breakers, 11 current transformers and 5 post insulators during Manjil (1990) earthquake [6]. The direct economic loss caused by Wenchuan (2008) earthquake estimated over 1 billion dollars and a total number of 246 substation suffered significant damages [7]. A substation equipment failure due to the Fukushima (2011) earthquake is displayed in Fig. 1.



Fig. 1. Damaged lightning arrester after Fukushima Earthquake (2011) [8].

Anchoring is a direct method to protect precision equipment from seismic vibration. Lopez and Soong [9] showed that seismic load could result in restraint breakage and excessive absolute acceleration. More recently, isolation technique has established as a design concept which decouples superstructure from ground shaking. The benefit of seismic isolation is to enhance superstructure safety and significantly reduce probable damages [10]. The period of isolator motion is longer than fixed base structure and the isolator period governs the fundamental period of isolated structure. As a result, the fundamental period of the structure shifts away from predominant periods of ground excitation thereby decreasing the energy imposed to the structure [11]. Substation facilities have several traits such as great rigidity, short natural period, and short displacement and other related traits. Therefore, period extension can be a solution to decrease exciting acceleration [12]. As a result, for the sake of strengthening the substation equipment, the use of isolation technology has the potential to become more prevalent.

Over the last decades, comprehensive research projects have been performed to investigate the effect of isolation technique in mitigating somehow irreparable damages to substation equipment by e.g. Sadeghvaziri *et al.* [13], Oikonomou *et al.* [14] and Murota *et al.* [15]. Although earthquakes are inevitable, the damage caused by earthquakes is not. This paper assesses the feasibility of isolation technique to lessen the seismic responses in terms of either structural or electrical requirements. Next, the effectiveness of the friction pendulum system (FPS), as a rehabilitation measure for a 2-item set of interconnected equipment including a Capacitor Voltage Transformer (CVT) and a Lightning Arrester (LA) is discussed.

## II. VERIFICATION OF MODELS

Since, it is intended to evaluate the simultaneous effect of the base isolation and the conductor interaction on seismic response of the aforementioned electrical equipment, it is necessary to model cable-connected equipped with FPS device. Based on general plan of "MontazerGhaem" substation, the 230 kV LA is installed next to the 230kV CVT at a distance of 3.5m. Therefore, the LA is modeled as well, which is interconnected to the CVT by a flexible conductor on a catenary configuration. Finite element model outputs were carefully scrutinized for the skewed results and then compared with the empirical data to insure that the resultant outputs were reasonable. The process by which modeling was performed is outlined in the following paragraphs.

### A. Substation Equipment:

Reaching the most precise values for an electrical equipment response, modeling process is carried out using finite element method. Fig. 2 and Fig. 3 display 3D finite element models of the CVT and LA.

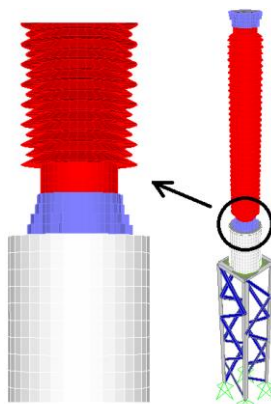


Fig. 2. Finite Element Model of Capacitor Voltage Transformer (CVT).

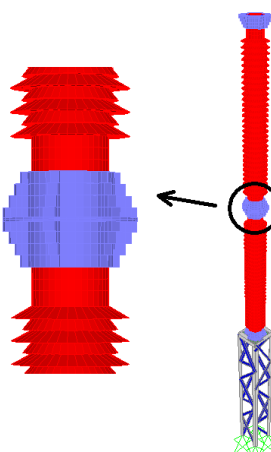


Fig. 3. Finite Element Model of Lightning Arrester (LA).

Brittle materials such as porcelain insulator (covering electrical parts) and cement fittings are considered to remain in elastic domain. An overview of the material specifications is provided in Table I.

**TABLE I- MECHANICAL PROPERTIES OF MATERIALS**

Material	Elastic Modulus (MPa)	Poisson Ratio
Aluminum	69000	0.33
Cement	25000	0.2
Porcelain	70000	0.24
Steel	210000	0.3

Structures carrying equipment include a 3D braced truss having 50cm in width. Although the higher altitude of structure will amplify equipment response, electrical clearance distance requirements allow minimum height of 250cm. The vertical members of structure are made of L60x60x6 angle while the diagonal members are made of L40x40x4 angle. Table II provides the height and mass of the equipment components.

**TABLE II- PARAMETERS OF THE MODELED EQUIPMENT**

Model	Height (cm)	Total Mass (kg)
CVT Structure	300	520
CVT Equipment	250	150
LA Structure	440	415
LA Equipment	250	150

Dynamic parameters of the aforementioned models should be rationally adjusted to the actual systems. The fundamental period of equipment models were calculated through modal analysis and compared to the ones stated in equipment catalog (Table III).

**TABLE III- MODELS VERIFICATION BY MODAL ANALYSIS**

Description	Natural Period (Catalog) (Sec.)	Natural Period (FEM) (Sec.)	Difference (%)
CVT (Equipment)	0.1124	0.1126	0.17
LA (Equipment)	0.1887	0.1859	1
CVT (on Structure)	0.1618	0.1631	0.8
LA (on Structure)	-	0.2398	N/A

In the first mode of isolated equipment which is called isolation mode and possess 99% of the total modal mass, the isolator undergoes deformation but the equipment behaves as essentially rigid. The natural period of this mode,  $T_1=1.03$  sec, indicates that the target period of isolation system,  $T_{eff}=1$  sec, is changed only slightly by flexibility of the equipment-structure system.

### B. Conductor:

Interaction of conductors between equipment subjected to earthquakes is a challenge for seismic design of substations [16]. Sufficient slack of flexible conductors allow them to accommodate the required relative displacement without excessive tension or compression [17]. To consider the required slack in conductor model, a nonlinear spring-dashpot system representing the flexible conductor is considered which the flexural rigidity and inertia effects were neglected. Based on the experimental test results, cable force-displacement diagram contains a range of linear elongation and a nonlinear behavior range where their flexibility diminishes abruptly (or their rigidity increases rapidly). Fig. 4 shows horizontal traction of a 1796 MCM conductor connection obtained from static cyclic test conducted by Dastous and Pierre [18] comparing to response of one corresponding finite element model.

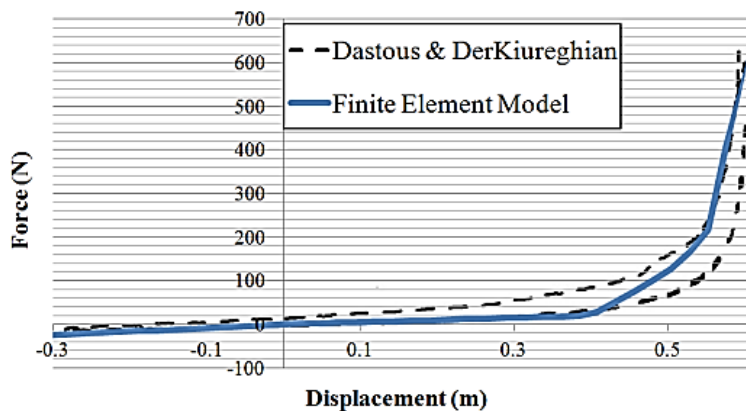


Fig. 4. Static Force-Displacement Behavior of the Model of Flexible Conductor against Test Result.

Furthermore, dynamic time history analysis is performed to ascertain the credit of dynamic response of the model. A cable-connected system consisting of two equipment items is subjected to the Northridge (1994) earthquake record [19]. The displacement time history of the second item is shown in Fig. 5. As it can be observed, the maximum dynamic characteristics of flexible conductor are captured accurately.

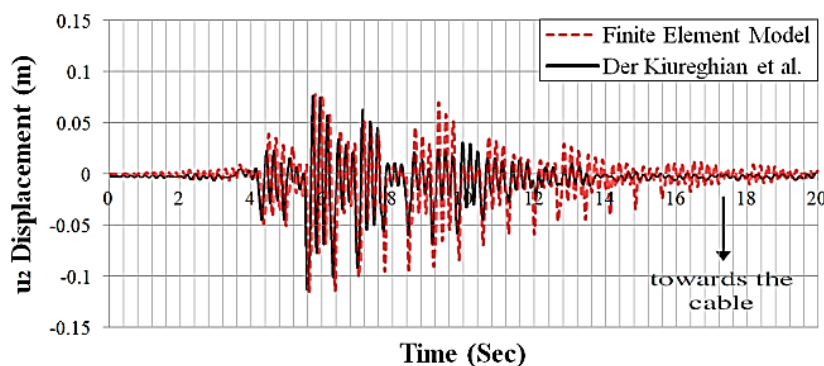


Fig. 5. Verification of displacement response for the second item.

The conductor used in this research is 1796-MCM with uniform distributed weight of

2.509 (kg/m) and Young's Modulus of  $5.72 \times 10^4$  MPa. Despite of probable quick use of slack and large tensions, catenary configuration is selected.

In this study, IEEE 693 [20] governs the method of defining the minimum length of conductor. IEEE 693 determines that if the PGA for 2% probability of exceedance in 50 years is greater than 0.5g, the high qualification level should be used. In addition, it recommends picking a damping value of 2% for substation equipment. In the light of these considerations, spectral acceleration ( $S_a$ ) is found from Required Response Spectrum (RRS). It should be noted that deflections obtained from the RRS must be multiplied by two in order to represent the behavior in a Performance Level earthquake which is 2 x RRS. Eventually, the minimum length of conductor is calculated as 392 cm and 400 cm for fixed-base and isolated-base conditions, respectively.

### C. Friction Pendulum System:

The base isolation device shall have sufficient restoring capabilities to return the equipment to its original position. Nevertheless, a modified isolation system called the friction pendulum system (FPS) possesses sliding and re-centering mechanisms integrated in one unit [21]. The weight independency property is the main FPS advantage that makes it suitable for lightweight apparatus such as substation structures [22]. The cross section of a single FPS is shown schematically in Fig. 6.

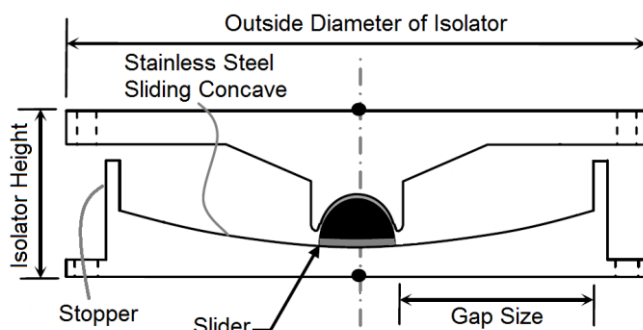


Fig. 6. Section view of a single Friction Pendulum System (FPS).

The gap size is one of the prominent variables considered in the present study. The rationale for the FPS design decision refers to its sensitivity to the displacement. Pounding of slider against stoppers seemed to be a matter of concern because of impulsive loading that may compromise function of the equipment or fracture the porcelain components.

The efficacy and functionality of FPS isolator is compromised by undesirable tensile or uplift forces which potentially entail detrimental effects on the superstructure. Using uplift-restraining isolator (such as XY-FPS isolator) could be a solution to the problem [23].

Force corresponding yield-displacement is a function of sliding surface material and gravity loads applied to bearing. By passing the yield point, friction behavior will be followed by sliding behavior. This leads to a combined friction-sliding action that forms

the nonlinear part of force-displacement diagram. As a result, the strength of friction pendulum system takes the following form:

$$F = \mu W \cdot \text{sgn}(u) + \frac{W}{R} u \quad (1)$$

where  $W$  represents the weight carried by isolator,  $R$  stands for sliding surface radius of curvature, and  $\mu$  is the friction coefficient of the bearing interface. Hysteretic behavior confirms that in order to define horizontal stiffness of the FPS, the frictional stiffness ( $\mu W$ ) or sliding stiffness ( $W/R$ ) should be determined. Besides, vertical stiffness of the single FPS device includes only compression stiffness of the articulated slider which is mostly made of stainless steel.

A two-level approach is used to design the FPS bearing: The Design Basis Earthquake (DBE) is taken as 5% probability exceeded in 50 years (975-year return period earthquake) and the Maximum Considered Earthquake (MCE) which has a 2% probability of being exceeded in 50 years (2475-year return period earthquake). The one-second spectral acceleration of site spectrum (5% of damping) for DBE and MCE are  $S_{D1}=0.46g$  and  $S_{M1}=0.57g$ , respectively. Since the FPS bearing design is aimed for 20% of damping, spectral acceleration values are multiplied by 0.8 [24].

The minimum friction coefficient shall meet the required force to stand against horizontal service loads which is mainly the wind load. Additionally, to compensate the low weight of equipment and make isolator installation possible, a  $1.5 \text{ m} \times 1.5 \text{ m} \times 0.4 \text{ m}$  concrete platform is considered between the bearings and the base of structure which is illustrated in Fig. 7. It is noteworthy that due to the symmetrical installation of isolators, mass eccentricity is negligible.

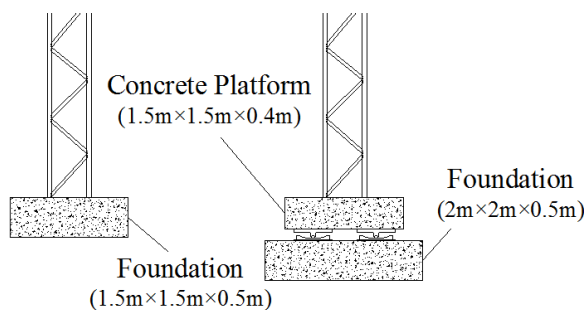


Fig. 7. Schematic view of concrete platform level and foundation level.

Due to summarize the design procedure of the FPS isolator, values of some other required parameters are presented in Table VI.

TABLE VI- SUMMARY OF FPS DESIGN PARAMETERS

Parameter	Quantity
Gravity Load	2840 (kg)
Dynamic Wind Loading	350 (kg)
Minimum Coefficient of Friction	0.08
Teflon-Stainless Steel	0.07-0.18

Buckle *et al.* [25] expressed that friction coefficient in the first cycle is approximately 20% greater than the value of average friction coefficient in all next cycles of displacement. AASHTO 2010 Guide [26] considers two main property modification factors during the life of the isolator. The minimum modification factor ( $\lambda_{\min}$ ) that is suggested to be assumed equal to one and the maximum property modification factor that is calculated 1.32. Therefore, the maximum probable friction coefficients is:

$$\mu_{\max} = \mu_{\min} \times 1.2 \times 1 \times 1.32 = 0.12 \quad (2)$$

Since the assumed effective period and damping values do not match at the deformation demand observed in the analysis, an iterative procedure is required [27]. The process commences with the assumption of effective period and effective damping ratio. The iterative design approach is applied as per AASHTO 2010 [26]. The converged quantity for target displacement of DBE is 8.1 cm. Hence, the gap size showed in Fig. 6 is equal to 8.1 cm for design of FPS.

### III. ANALYSIS

To consider the dynamic response of high-voltage electrical equipment, triaxial nonlinear time history analysis is carried out. The IEEE 693 advises to apply ground motions simultaneously in the two perpendicular horizontal axes and the vertical axis, which 80% of that is in the horizontal axes. Furthermore, orthogonal equipment response shall be calculated through SRSS method.

According to the IEEE 693, load combination is decided to be based on the LRFD design methodology as follows:

$$LRFD : 1.2D + 1.4E_{RSS} + OP \quad (3)$$

where D is dead load,  $E_{RSS}$  denotes the earthquake load demand from the service load, and OP shows operating load such as short circuit force and tension induced by conductor weight.

#### A. Ground Motions:

Twenty recorded components of far-field earthquake ground motion on very dense soil and soft rock (Class C sites as defined by ASCE 7-05 [28]) are selected. The specifications of picked ground motions are summarized in Table V. The spectrum of selected ground motions comparing to normalized response spectrum of the IEEE 693 (bold lines) is illustrated in Fig. 8. Ground motions are selected from the PEER database and an attempt is made to avoid any resemblance to the pulse-like records.

TABLE V- SELECTED GROUND MOTIONS

Earthquake	Station	Distance (km)	PGA (g)
Cape Mendocino	89324 Rio Dell Overpass – FF	18.5	0.385
Chi Chi	TCU047	33.01	0.413

Chi Chi (2)	CHY074	82.49	0.234
Coalinga	36449 Parkfield - Fault Zone 8	29.6	0.131
Imperial Valley	6604 Cerro Prieto	26.5	0.169
Kern County	283 Santa Barbara Courthouse	87	0.127
Kocaeli	Goynuk	35.5	0.132
Kocaeli (2)	Arcelik	17	0.218
Landers	21081 Amboy	22.5	0.171
Loma Prieta	57504 Coyote Lake Dam(Downst)	21.7	0.179
Loma Prieta (2)	1652 Anderson Dam (Downst)	21.4	0.24
Morgan Hill	57007 Corralitos	22.7	0.109
Morgan Hill (2)	57383 Gilroy Array	11.8	0.292
Northridge	90021 LA - N Westmoreland	29	0.401
Northridge (2)	90015 LA - Chalon Rd	23.7	0.225
San Fernando	24278 Castaic - Old Ridge Route	24.9	0.324
Trinidad	1498 Rio Dell Overpass, FF	71.9	0.147
Victoria	6604 Cerro Prieto	34.8	0.621
Westmorland	5051 Parachute Test Site	24.1	0.242
Whittier Narrows	24157 LA - Baldwin Hills	27	0.142

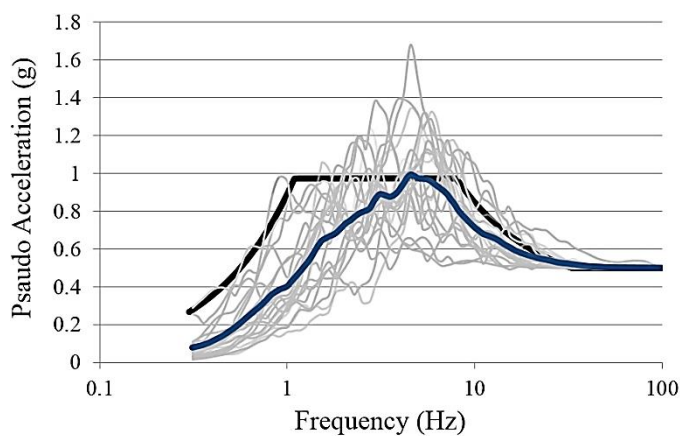


Fig. 8. Average of input ground motion spectrum compared to normalized response spectrum of IEEE Std. 693.

### B. Failure Mechanisms:

Reports on failure due to the porcelain insulator breakage outnumber any other reported failure modes of the CVT and LA. Therefore, this study focuses on the flexural breakage of porcelain as the main failure mode. Since the material of porcelain is considered as unglazed aluminous porcelain (C120), the ultimate bending stress is 500 kg/cm<sup>2</sup> [31]. The IEEE 693 stipulates that porcelain loads/stresses shall not exceed 50% of the ultimate load/stress of the porcelain [20].

The breakage of fittings at the end of flexible conductor is noticed as the second failure mode. The IEEE 1527 [32] explains that at high qualification level, the value of the maximum load, which each terminal pad is designed to subject to, should be 200 kg. In addition, relying on the base isolation strategy should not result in electrical clearance problems. Safety clearance zone is consisted of two phase-ground

clearances and the distance between bottom of conductor and substation ground (Fig. 9).

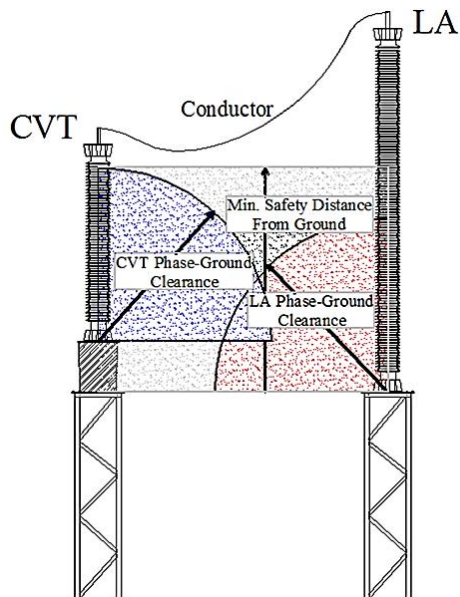


Fig. 9. Schematic view of the 2-item set of equipment and main safety clearances compared to the shape of flexible conductor.

As stated by ANSI C37.32 [33] for a 230 kV substation and BIL of 1050 kV, ground clearance should be maintained at 5m and the minimum earth clearance value should not exceed 2.1 m. Since horizontal moving of terminals toward each other can possibly lead to the violation of conductor to the displayed zone in the previous figure, they should be monitored not to exceed 40 cm.

### C. Incremental Dynamic Analysis:

Incremental Dynamic Analysis (IDA) includes a nonlinear dynamic time history analysis that is an applicable method to better understand the changes of response known as Demand Measure (DM) versus those of increased ground motion intensity known as Intensity Measure (IM) [29].

To choose the IM for lightweight isolated apparatus, the PGA is most likely not the best indicator of their performance [30]. Therefore, it is decided in the present study that the peak ground displacement (PGD) can more effectively represent the seismic response among all other alternative measures. Moreover, two failure modes mentioned above (allowable stress at the base of porcelain insulator and allowable force at the terminal pads) are selected as the DM.

The IDA method needs every ground motion record to be scaled incrementally until one of the defined failure criteria is achieved. Afterwards, the IDA is performed for several scaling levels of twenty ground motions each normalized by the PGD of 3 cm to a PGD of 30 cm in increments of 3 cm.

#### IV. RESULTS

The IDA curves of the non-isolated 2-item set of equipment are presented in Fig. 10 and Fig. 11. It is noteworthy that the failure boundary is displayed by a vertical dashed line which represent porcelain breakage (as the obtained dominant failure mode). The bold line shows the median response. As implied below, it can be concluded that the LA porcelain breakage occurs in a smaller value of the PGD which means the LA is much more susceptible to failure.

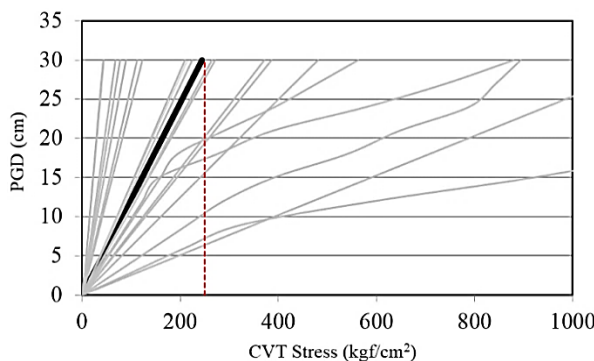


Fig. 10. Stress at the bottom of CVT porcelain insulator against PGD.

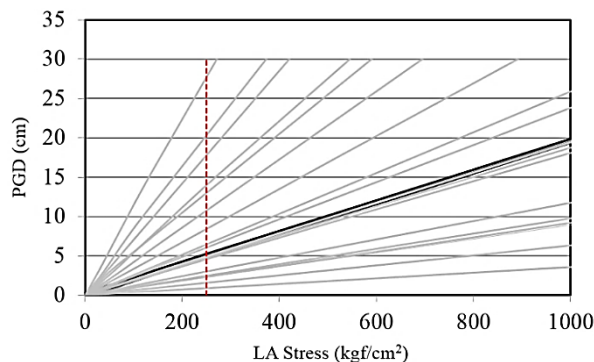


Fig. 11. Stress at the bottom of LA porcelain insulator against PGD.

##### A. Effect of isolation:

To evaluate the isolation effect on the seismic performance of the 2-item set of equipment, two different cases are investigated:

- A. Base isolation of the CVT while the LA is fixed-base and
- B. Base isolation of the LA while the CVT is fixed-base.

The following figures present a comparison of median responses between fixed-base set of equipment, case A and case B. As it can be inferred from Fig. 12, by exceeding a threshold of PGD, the larger intensity of excitation introduces adverse functionality of isolated-base CVT comparing fixed-base one. The PGD corresponding porcelain breakage suggests that isolated-base CVT suffers from the lack of seismic resistance in case A.

On the other hand, Fig. 13 presents no difference in the way fixed-base and isolated-

base LA responses. Therefore, base isolating of the CVT (case A) cannot enhance seismic performance of 2-item set of equipment and leads to malfunction of isolation plan.

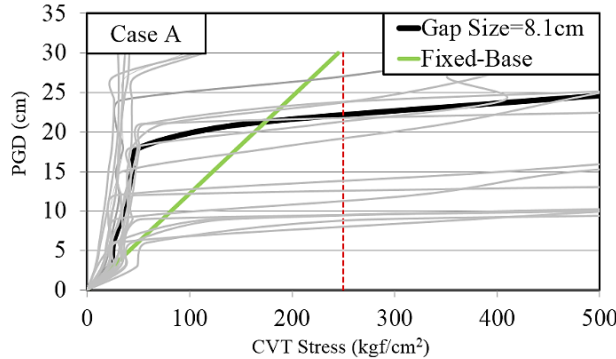


Fig. 12. Stress of CVT porcelain corresponding Case A (Gap Size=8.1 cm).

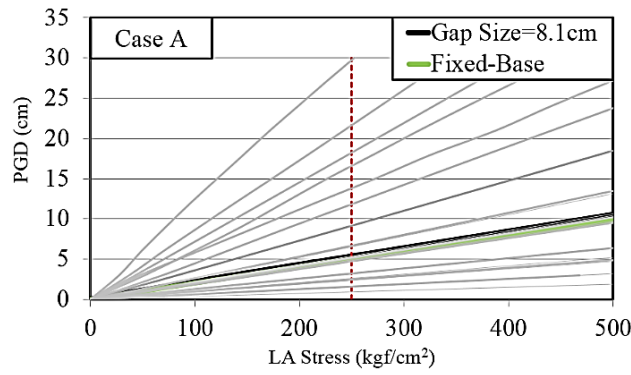


Fig. 13. Stress of LA porcelain corresponding Case A (Gap Size=8.1 cm).

Unlike, Fig. 14 and Fig. 15 show that isolated-base LA is much more appropriate than fixed-base one in case B, which satisfies stress requirements in both the CVT and LA at all the PGDs. This implies that the LA isolating plan postpones both the LA and CVT failures and seismic strengthening is achieved.

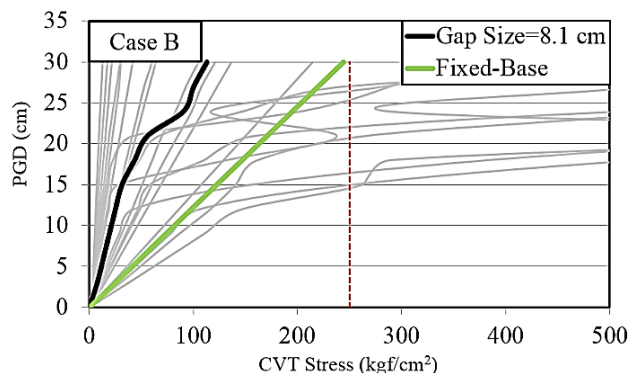


Fig. 14. Stress of CVT porcelain corresponding Case B (Gap Size=8.1 cm).

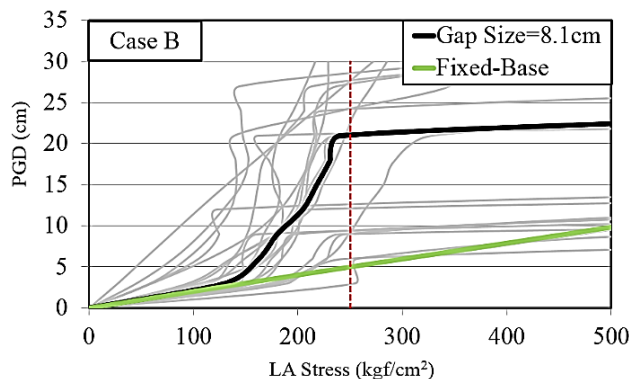


Fig. 15. Stress of LA porcelain corresponding Case B (Gap Size=8.1 cm).

The median values of load at terminal pads are presented in Fig. 16 and Fig. 17. As shown below, terminal pads will break for gap sizes of 15 cm and higher in case A, while case B results in smaller loads and it never pass the allowable force. So, it can be easily deduced that plan of base-isolating the LA (case B) is more reasonable.

Comparing all the aforementioned figures, the seismic performance of case B (FPS at the base of the vulnerable equipment) is found more suitable than case A. Moreover, the figures approve that the failure following terminal pads breakage seldom happens. Consequently, regarding the porcelain breakage as the main concern is acceptable.

As a result, case B can be a solution to the problem of porcelain breakage.

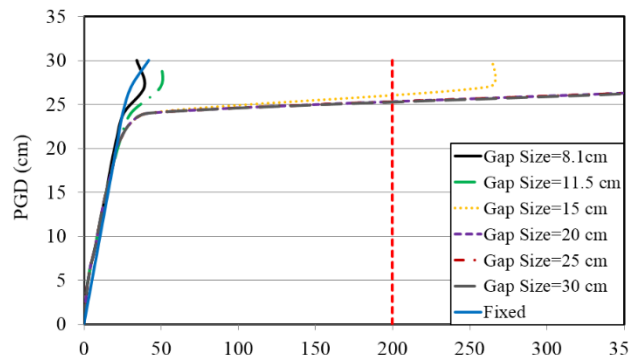


Fig. 16. The median values of terminal pads forces for Case A.

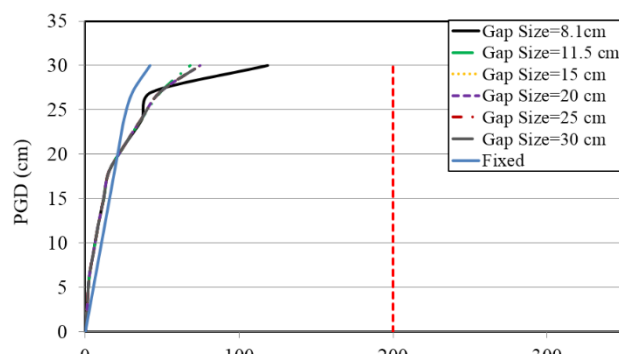


Fig. 17. The median values of terminal pads forces for Case B.

It is worth mentioning that the median values of relative displacement between

terminal pads never exceed the specified criterion for safety clearance. Hence, proper operation and integrity of the facility and safety is ensured. Note that no sign of overturning is seen and thereby, uplift phenomena cannot be a concern.

### B. Effect of gap width:

Since the PGD is taken as the IM, pounding of slider against stoppers is a matter of concern. Therefore, the influence of the gap between stoppers presented in Fig. 6 is one of the most prominent variables considered in the present study. As a result, different gap sizes are selected as 8.1 cm (for DBE), 11.5 cm (for MCE), 15 cm, 20 cm, 25 cm and 30 cm. Fig. 18 and Fig. 19 illustrate the effect of different chosen gap sizes on the porcelain response. As shown below, the larger the gap sizes, the less is the stress in porcelain.

It can be concluded that sudden increase of porcelain stress corresponds a specified PGD which is a result of pounding effect.

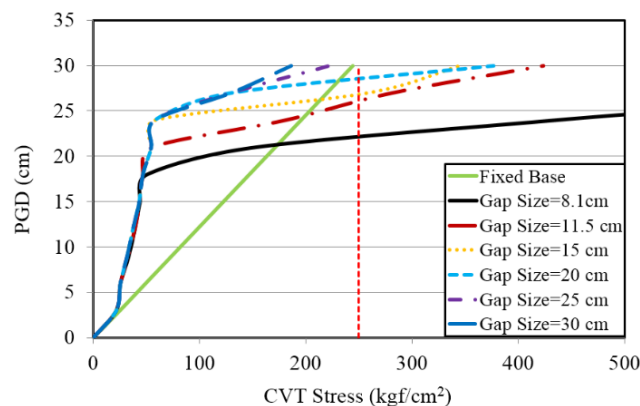


Fig. 18. Stress of CVT porcelain corresponding Case A (different gap sizes).

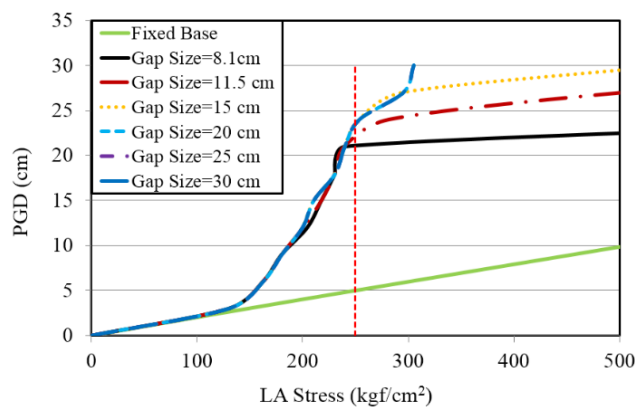


Fig. 19. Stress of LA porcelain corresponding Case B (different gap sizes).

### C. Fragility Curve:

Fragility functions are probability distributions used to determine the probability which an element or system will incur a given amount of damage during a seismic event. The

fragility curves are derived from ATC 58 [34], which lays out the specific guidelines for developing fragility curves; they all take the form of lognormal cumulative distribution functions.

We use the lognormal since it fits a variety of nonstructural components failure data well [35]. The mathematical form of fragility function is:

$$F_i(D) = \Phi\left(\frac{\ln(D/\theta_i)}{\beta_i}\right) \quad (4)$$

where  $F_i(D)$  represents the conditional probability that the component will be damaged in damage state "i",  $\Phi$  stands for the standard normal (Gaussian) cumulative distribution function,  $D$  is demand parameter,  $\theta_i$  denotes median value and  $\beta_i$  denotes logarithmic standard deviation or dispersion. Due to treating different types of failure mechanisms similarly,  $D$  is defined as the ratio of the maximum response ( $d_{imax}$ ) to the failure response ( $d_{failure}$ ):

$$D = \frac{d_{imax}}{d_{failure}} \quad (5)$$

Clearly, damage will occur when for each damage state (i),  $D$  exceeds unity. It should be noted that both  $\theta$  and  $\beta$  are established for the PGDs corresponding to  $D=1$ . The fragility curves are developed using two aforementioned cases A and B. In addition, fragility curves identified for the damage state of fixed-base apparatus and isolated-base configuration including different gap sizes. The fragility curves for two aforementioned cases are displayed in Fig. 20 and Fig. 21.

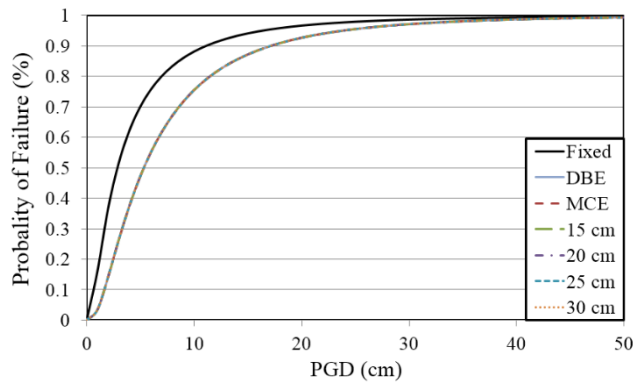


Fig. 20. Fragility functions of 2-item set of equipment (Case A).

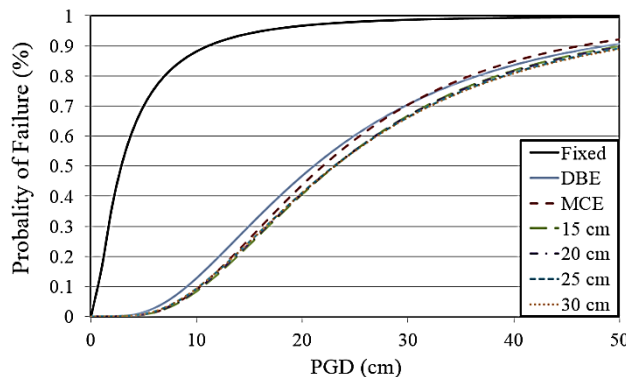


Fig. 21. Fragility functions of 2-item set of equipment (Case B).

As shown above, comparing fragility curves provides the proof that installation of friction pendulum system at the base of LA is more suitable in order to decrease failure likelihood of the 2-item set of equipment. Besides, comparing the different damage states of fragility functions suggests that increasing the stoppers gap sizes will not reduce failure chance of the 2-item set of equipment. However, seismic responses of equipment are improved by widening the gap between the FPS stoppers.

## V. CONCLUSION:

In this paper, an analytical study is implemented in order to improve seismic performance of a 2-item set of substation equipment. Seismic response is assessed by incremental dynamic analysis with respect to scaled PGD that is deemed acceptable. Thereafter, the fragility function is developed through a two-pronged approach: equipping the CVT and then the LA with the friction pendulum system. The main conclusions are:

- Although using the FPS for the CVT lessen the porcelain stress of its own, it cannot assist in mitigating the response of the 2-item set of equipment since the failure of LA porcelain is prior to that of the CVT. Besides, passing a threshold of PGD, causes a surprisingly adverse effect of isolated-base CVT comparing with fixed-base one.
- Seismic response of fixed-base 2-item set of equipment draws a conclusion that the LA is more susceptible to failure. Consequently, if the friction isolator is installed at the base of the LA, equipment safety considerably enhances so that the failure likelihood noticeably decreases. This satisfies the strengthening which is not possible through the first method.
- Despite that the seismic safety of base-isolated equipment (lightweight components) can be increased by widening the gap between the FPS stoppers, it does not notably affect failure probability of 2-item set of equipment (Fig. 18-Fig. 21).

## VI. REFERENCES

- [1] C. Stearns and A. Filiatrault, "Electrical Substation Equipment Interaction: Experimental Rigid Conductor Studies," *Pacific Earthquake Engineering Research Center (PEER)*, California, USA, 2005.
- [2] A. Hashemi Nezhad Ashrafi, "Issues of Seismic Response and Retrofit for Critical Substation Equipment," Department of Civil and Environmental Engineering, M.S. thesis, New Jersey Institute of Technology, 2003.
- [3] T. Anagnos, "Development of an Electrical Substation Equipment Performance Database for Evaluation of Equipment Fragilities," *Pacific Earthquake Engineering Research Center (PEER)*, 1999.
- [4] ASCE 96, Maunals and Report on Engineering Practice. Guide to Improved Earthquake Performance of Electric Power Systems., ASCE (American Society of Civil Engineering), 1999.
- [5] M. Erdik, "Report on 1999 Kocaeli And Duzce (Turkey) Earthquakes," Bogazici University, Dept. of Earthquake Engineering, Istanbul, Turkey, 1999.
- [6] "Damage report of Shahid Beheshti power plant in 1990 earthquake," Tavanir, Iran, 1990.
- [7] R.S. Liu, M.J. Zhang and Y.B. Wu, "Vulnerability Study of Electric Power Grid in Different Intensity Area in Wenchuan Earthquake," in *15th World Conference of Earthquake Engineering (WCEE)*, Lisboa, Portugal, 2012.
- [8] "Report Regarding Collection of Reports pursuant to the Provisions of Article 106, Paragraph 3 of the Electricity Business Act," Tokyo Electric Power , May 2011.
- [9] G.D. Lopez, T.T. Soong, "Sliding Fragility of Block-Type Nonstructural Components. Part 1: Unrestrained Components," *Earthquake Engineering Structures Dynamic*, vol. 32, no. 1, pp. 131-149, 2003.
- [10] A. Charles and P.E. Kircher, "Chapter 12: Seismically Isolated Structures," FEMA P-751, NEHRP Recommended Provisions: Design Examples, 2012.
- [11] P. Murnal and R. Sinha, "Aseismic design of structure–equipment systems using variable frequency pendulum isolator," *Nuclear Engineering and Design*, vol. 231, pp. 129-139, 2004.
- [12] B. Wen, J. Zhang and D. Niu, "Application of Isolation Technology in High-voltage Electrical Equipments," in *The 14th World Conference on Earthquake Engineering*, Beijing, China, October 2004.
- [13] M. Ala Saadeghvaziri, B. Feizi, L. Kempner and D. Alston, "On Seismic Response of Substation Equipment and Application of Base Isolation to Transformers," *IEEE Transactions on Power Delivery*, vol. 25, no. 1, pp. 177 - 186, Jan 2010.
- [14] K. Oikonomou, M.C. Constantinou and A. M. Reinhorn, "Seismic Isolation of Electrical Equipment "Seismic Table Simulation"," in *15th World Conference of Earthquake Engineering*, Lisbon, Portugal, 2012.
- [15] N. Murota, M.Q. Feng and Y.L. Gee, "Experimental and Analytical Studies of Base Isolation Systems for Seismic Protection of Power Transformers," MCEER, Federal Highway Administration, 2005.
- [16] J. B. Dastous and A. Der Kiureghian, "Application Guide for the Design of Flexible and Rigid Bus Connections between Substation Equipment Subjected to Earthquakes," *Pacific Earthquake Engineering Research Center (PEER)*, California, USA, 2010.

- [17] H. Ghalibafian, "An Experimental Study on the Seismic Interaction of Flexible Conductors with Electrical Substation Equipments," M.S. thesis, Department of Civil Engineering, The University of British Columbia (UBC), Vancouver, Canada, 2001.
- [18] J. B. Dastous and J. R. Pierre, "Experimental Investigation On The Dynamic Behavior Of Flexible Conductors Between Substation Equipment During An Earthquake," IEEE Transactions on Power Delivery, vol. 11, no. 2, pp. 801-807, April 1996.
- [19] A. DerKiureghian, J. L. Sackman and K. J. Hong, "Interaction in Interconnected Electrical Substation Equipment Subjected to Earthquake Ground Motions," Pacific Earthquake Engineering Research Center (PEER), California, USA, 1999.
- [20] IEEE 693-Recommended Practice for Seismic Design of Substations, The Institute of Electrical and Electronics Engineers (IEEE), 2005.
- [21] V.A. Zayas, S.S. Low and S.A. Mahin, "A simple pendulum technique for achieving seismic isolation," *Earthquake Spectra*, vol. 6, p. 317–333, 1990.
- [22] G.P. Warn and K.L. Ryan, "A Review of Seismic Isolation for Buildings: Historical Development and Research Needs," *Buildings*, vol. 2, pp. 300-325, 2012.
- [23] C. Panayiotis and M. Roussis, "Study on the Effect of Uplift Restraint on the Seismic Response of Base-Isolated Structures," *Journal of Structural Engineering*, pp. 1462-1471, 2009.
- [24] M. J. N. Priestley, "Myths and Fallacies in Earthquake Engineering," in *The Mallet Milne Lecture*, IUSS Press, Istituto Universitario di Studi Superiori di Pavia, Pavia, Italy, 2003.
- [25] I. G. Buckle, M. C. Constantinou, M. Dicleli and H. Ghasemi, "Seismic Isolation of Highway Bridges," MCEER, Federal Highway Administration, 2006.
- [26] Revised AASHTO guide specifications for seismic isolation design, American Association of State Highway Transportation and Officials (AASHTO), Washington DC, 2010.
- [27] B. D. Richins, "Evaluation and Seismically Isolated Substructure Redesign of a Typical Multi-Span Pre-Stressed Concrete Girder Highway Bridge," Utah State University, Civil and Environmental Engineering, M. S. thesis, Utah, 2011.
- [28] "ASCE 7-05: Minimum Design Loads for Buildings and Other Structures," American Society of Civil Engineers (ASCE), 2005.
- [29] D. Vamvatsikos and C. Cornell, "Incremental Dynamic Analysis," *Earthquake Engng Struct. Dyn*, pp. 1-23, 2002.
- [30] H. Akiyama, Earthquake-resistant limit-state design for buildings, Tokyo, Japan: University of Tokyo Press, 1980.
- [31] IEC 60672-3: Ceramic and Glass Insulating Materials-Part3: Specifications for Individual Materials, International Electrotechnical Commission (IEC), 1997.
- [32] IEEE Recommended Practice for the Design of Flexible Buswork Located in Seismically Active Areas, IEEE Standard 1527, 2006.
- [33] High-Voltage Air Disconnect Switches Interrupter Switches, Fault Initiating Switches, Grounding Switches, Bus Supports and Accessories Control Voltage Ranges-Schedules of Preferred Ratings, Construction Guidelines and Specificat, American National Standard (ANSI C37.32), 1996.

- [34] ATC 58-Guidelines for Seismic Performance: Assessment of Buildings, Applied Technology Council (ATC), Washington D.C., USA, 2007.
- [35] K.M. Porter and A.S. Kiremidjian, "Assembly-Based Vulnerability and its Uses in Seismic Performance Evaluation and Risk-Management Decision-Making," John A. Blume Earthquake Engineering Center, Stanford, CA, 2001.